Printed UWB Pacman-Shaped Antenna with Two Frequency Rejection Bands

Shaimaa' Naser and Nihad Dib

Department of Electrical Engineering
Jordan University of Science and Technology, P. O. Box 3030, Irbid 22110, Jordan
naser.shaimaa@yahoo.com, nihad@just.edu.jo

Abstract ─ In this paper, the design and analysis of microstrip-fed low-profile, compact ultra-wideband (UWB) monopole antenna with two band-notches characteristics is carried out. The antenna is mounted on a low-cost FR-4 substrate with dimensions of 25×38×1.6 mm^3, and relative permittivity of 4.4. The original shape of the patch is circular with radius of 11.5 mm, and then a sector is removed from the patch (making it a *Pacman*-shaped antenna) to improve the impedance bandwidth. The proposed antenna provides an impedance bandwidth between 2.9-15 GHz with better than 10 dB return loss and has nearly an omni-directional radiation pattern. Additionally, the antenna can reject the interference from WiMAX (3.5 GHz center frequency) and WLAN (5.5 GHz center frequency).

Index Terms ─ Monopole antennas, notch filters, ultra wideband antennas.

I. INTRODUCTION

Nowadays, Ultra-wideband (UWB) technology is widely used due to its capability of transmitting high data rates through the large bandwidth it utilizes. UWB technology is suited for systems that use short range communications and high data rates. Such systems include: radar applications, sensor data collection, precision locating, wireless sensor networks, ad-hoc networks and tracking applications. Federal communications commission (FCC) has adopted the band 3.1-10.6 GHz for the UWB signal and power spectral density emission limit for UWB transmitters of −41.3 dBm/MHz [1].

One of the most important parts of an UWB system is the antenna. The design of UWB antennas must ensure high radiation efficiency, low cost, and small size. There are many types of UWB antennas in the literature, but, recently, most researchers have been focusing on the design of printed monopole antennas since they have broad bandwidth, low cost, and low profile. Since the adoption of the FCC, many studies have been made on the design and performance of UWB antennas [2-8].

UWB signals can introduce interference with common wireless technologies such as WiMAX (3.5 GHz) and WLAN (5.5 GHz). So, another key design issue is to reject the interference from such technologies. Different methods have been used for designing the notch filters such as inserting slots either on the patch, the ground, or on the feeding line [9-17]. This method is very simple and does not add any overhead on the antenna structure but, using this method, it is difficult to achieve narrow band-stop region. Another method includes inserting parasitic elements that provide current flowing in opposite directions at the notch frequency [18]. Although this method increases the size of the antenna, it can achieve very narrow band stop regions.

The rest of the paper is organized as follows: Section II describes the design procedure of the proposed antenna and the optimum design parameters. Section III describes the antenna characteristics. Section IV presents a parametric study of several design parameters that affect the antenna performance. Finally, Section V concludes and summarizes the study.

II. ANTENNA DESIGN

Figure 1 illustrates the geometry of the proposed *Pacman*-shaped printed microstrip-fed UWB antenna. The antenna is mounted on a compact size FR-4 substrate of dimensions 25 mm× 38 mm, dielectric constant 4.4, loss tangent of 0.02, and thickness of 1.6 mm. The original patch has circular shape since it has the largest bandwidth among the other regular shapes and has good radiation characteristics [19]. The radius was approximated to be λ/4 at the lower frequency edge of the UWB range as follows [20]:

$$R = \frac{c}{4 f_l \sqrt{\varepsilon_r}}, \quad (1)$$

where R is the patch radius, f_l is the lower frequency edge (i.e., 3.1 GHz), c is the free-space speed of light, and ε_r is the substrate dielectric constant. The feeding line has a length of 12 mm and a width of 3 mm to achieve a characteristic impedance of 50 Ω. From simulation, it has been found that the distance p ($p = L_{feeding} - W_{gnd}$) between the feeding point and the ground plane has an effect on the performance of the antenna. Its value was chosen to be 0.2 mm. A partial ground plane is used with a notch cut near the feeding line to improve the impedance bandwidth. The notch

Submitted On: July 24, 2016
Accepted On: January 28, 2017

1054-4887 © ACES

dimensions were varied to have good return loss; the optimum values chosen are W_1 = 0.8 mm and L_1 = 5 mm. Then, a sector was removed from the circular patch (making it a *Pacman*-shaped antenna) to improve the impedance bandwidth, and its angle was optimized to be 80° to have a good return loss and large bandwidth. Finally, a U-shaped slot and a straight slot were etched in the patch to reject the interference from WiMAX and WLAN, respectively. The total lengths of the slots were approximated to be λ/2 at the notched frequencies [12-14]:

$$L_{notch} = \frac{c}{2 f_{notch}\sqrt{\varepsilon_{eff}}}, \quad (2)$$

where f_{notch} is the center frequency of the notched band, and $\varepsilon_{eff} = \frac{\varepsilon_r+1}{2}$.

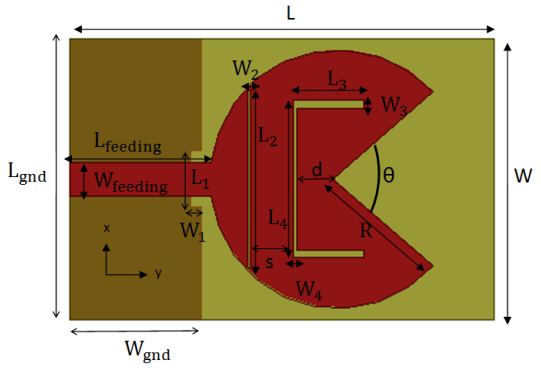

Fig. 1. The layout of the proposed *Pacman*-shaped antenna.

To model and optimize the proposed antenna, HFSS simulator was used. A radiation box placed at a distance of $\lambda/4$ from the substrate was used to measure the far field parameters. The solution frequency was set to 3.1 GHz which is the lowest frequency edge, with maximum delta S = 0.01 and number of passes of 12. After several simulations and performing a parametric study (described in Section IV), the optimum parameters of the proposed UWB antenna are chosen as follows:
L = 38 mm, W = L_{gnd} = 25 mm, $L_{feeding}$ = 12 mm, $W_{feeding}$ = 3 mm, W_{gnd} = 11.8 mm, R = 11.5 mm, W_1 = 0.8 mm, L_1 = 5 mm, W_2 = 0.2 mm, L_2 = 15.8 mm, W_3 = 0.7 mm, L_3 = 6mm, W_4 = 0.3 mm, L_4 = 14 mm, θ = 80°, S = 3.8 mm, and d = 3.1 mm.
The optimum design parameters were used to build a prototype of the proposed antenna which is shown in Fig. 2.

Measurements were performed in the laboratory environment using an Agilent Vector Network Analyzer (VNA). Figure 3 shows the simulated and measured voltage standing wave ratio (VSWR) of the proposed antenna. It can be observed that measurement agrees well with simulation except in the range 11-13 GHz which could be due to experimental tolerances, fabrication tolerances, and the effect of the connector. The antenna works in the UWB range with the VSWR being less than 2 in the frequency band 2.9-15 GHz except around the notched frequencies. As desired, the antenna has filter characteristics around 3.5 GHz (the center frequency of WiMAX) and 5.5 GHz (the center frequency of WLAN). A small shift in the measured notched frequencies can be noticed because the simulation environment is different from the real environment, and the fact that the substrate relative permittivity decreases as the frequency increases [21]. Similar shifts in the notched frequencies were seen in other papers for the same causes [10], [11], [16].

Fig. 2. Picture of the fabricated *Pacman*-shaped UWB antenna.

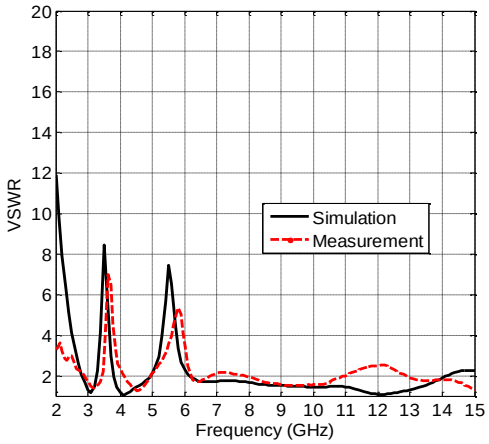

Fig. 3. The simulated and measured VSWR of the antenna.

III. ANTENNA PARAMETERS

This section elaborates more on the proposed antenna parameters. Since UWB antennas involve transmission of large bandwidths, time domain parameters are as important as the frequency domain parameters because they determine how much the antenna disperses the received signal. Different frequency domain parameters and the group delay for the proposed antenna will be discussed in this section.

A. Antenna gain

Usually, when one talks about the antenna gain, he/she refers to the realized peak gain which takes into account the mismatch losses. The simulated gain of the

antenna is illustrated in Fig. 4. The gain increases in the whole antenna bandwidth from 2 dB to nearly 8 dB, while it drops to -5.4 dB at 3.5 GHz (the center frequency of WiMAX) and to -2.9 dB at 5.5 GHz (the center frequency of WLAN).

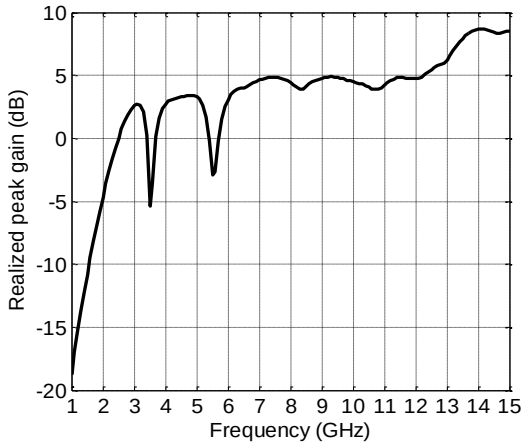

Fig. 4. The realized peak gain of the antenna

B. Radiation pattern

UWB printed monopole antennas are known to have omni-directional pattern similar to the linear monopole antenna in which the E-plane has the figure-8 shaped pattern, and the H-plane is non-directional. Moreover, an antenna can have two polarizations, one is in the intended direction (co-polarization), and the other is orthogonal on it (cross-polarization) [22]. One should try to minimize the cross-polarization to reduce polarization mismatch. Figure 5 illustrates the E-plane (yz-plane) and H-plane (xz-plane) co-polarization and cross-polarization patterns of the antenna at 4, 6, and 9 GHz.

It is clear that the antenna has the figure-8 shape in the E-plane with very small cross-polarization component, but as the frequency increases, the radiation pattern becomes distorted and the cross-polarization component increases. On the other hand, the antenna is non-directional (having an O-shaped pattern) in the H-plane with cross-polarization component lower than the co-polarization one.

C. Current distribution

The last frequency domain parameter to consider is the current distribution. Figure 6 illustrates the current distribution at 3.5, 5.5, 9, and 12 GHz. It can be observed that the current is mainly concentrated at the edges of the circular patch and the feeding line, but, this does not happen at 3.5 GHz where the current is mainly concentrated at the U-shaped slot (WiMAX slot) and 5.5 GHz where the current is mainly concentrated at the WLAN straight slot. This indicates that the notches have a short circuit effect to prevent interference from WLAN and WiMAX.

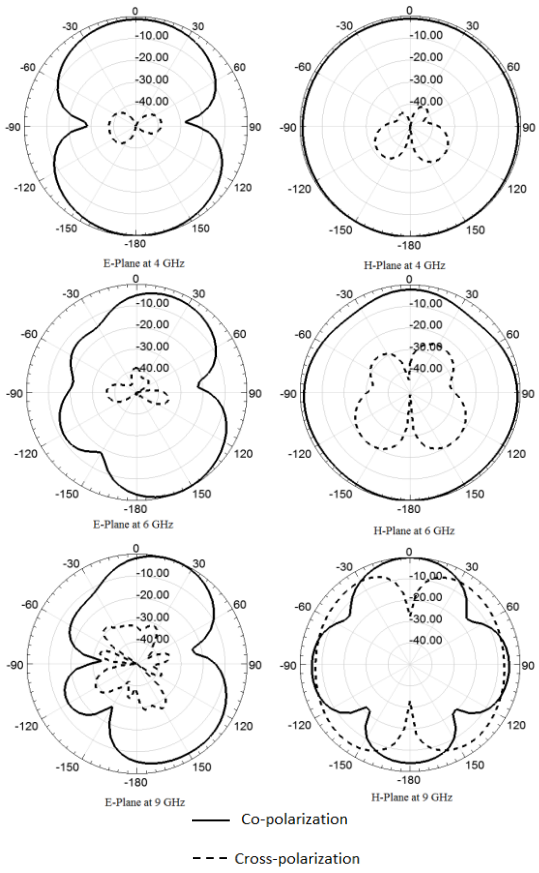

Fig. 5. The normalized E-plane and H-plane co-polarization and cross-polarization patterns (in dB) at 4, 6, and 9 GHz.

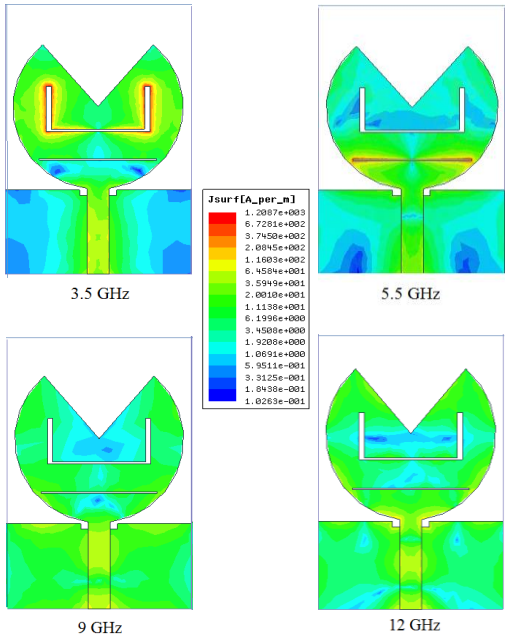

Fig. 6. The current distrbution at 3.5, 5.5, 9, and 12 GHz.

D. Group delay

Group delay has an important role in the dispersion characteristics of the antenna. A comparison between the simulated group delay (using S_{11} and S_{21}) and the measured one (computed using the measured S_{11}) is illustrated in Fig. 7. To compute the group delay from the phase of S_{21}, two similar proposed antennas were placed face-to-face a distance of 30 cm. The group delay is almost constant over the whole band except at the notched frequencies. In fact, using S_{21} to compute the group delay gives more realistic results. Since the measured group delay is almost constant, little distortion is introduced by the antenna.

Table 1 lists a comparison between the proposed antenna and six other ones that have recently appeared in literature. It can be seen that the proposed design has a comparable size compared to others, with a larger peak gain. Moreover, the low and high frequency edges compete with the ones cited in the table.

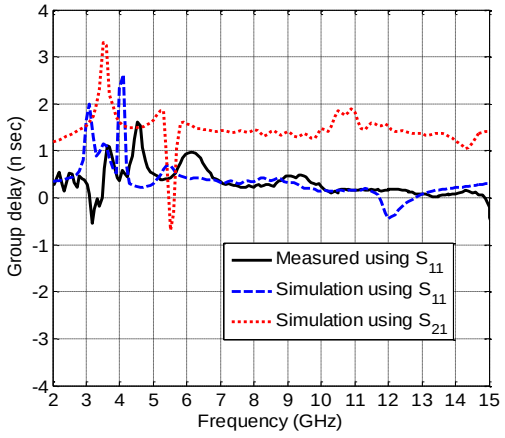

Fig. 7. The simulated and measured group delay of the proposed antenna.

Table 1: Comparison between the proposed design and previous designs

Ref.	Dimension	Peak Gain (dB)	f_l (GHz)	f_H (GHz)
[8]	12 mm × 18 mm	6	2.8	11.6
[17]	42 mm × 40 mm	4.4	2.44	11.9
[9]	25 mm × 20 mm	3	2.63	13.02
[2]	29 mm × 20.5 mm	6	3	10.72
[23]	41 mm × 34 mm	4.85	3.26	19.1
[24]	63.25 mm × 51 mm	-	3.1	15
Proposed	38 mm × 25 mm	8	2.9	15

IV. PARAMETRIC STUDY

A parametric study of the proposed antenna was performed to control the antenna and the notch filters operations. The first parameter to consider is the effect of the angle of the sector on the antenna return loss (without the existence of the filtering slots) which is illustrated in Fig. 8. It is clear that the angle of the sector highly affects the return loss. As the angle is varied, the return loss and the input impedance change. So, a value that achieves a good return loss, good input impedance, and wide bandwidth was chosen to be 80°.

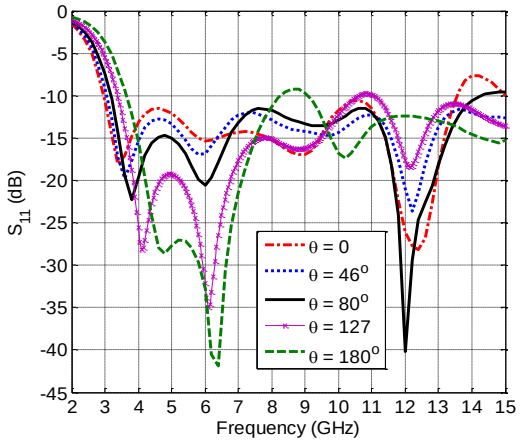

Fig. 8. The effect of varying the angle of the sector with R = 11.5 mm, p = 0.2 mm, and W_1 = 0.8 mm.

Then, the effect of the slots dimensions on the notched frequencies is studied. The notches lengths were initially computed to be λ/2 at the notch frequencies, and then their widths, lengths, and positions (S and d) were optimized. Figures 9, 10, and 11 show the effect of varying the widths of the notches W_2, W_3, and W_4, respectively, while keeping the radius, the gap *p*, the ground plane notch dimensions, and the sector angle fixed to the optimum values. From Fig. 9, it can be seen that changing W_2 has no effect on the center frequency of the WiMAX, while it changes the center frequency of the WLAN. Its value was set to 0.2 mm to have the center frequency at 5.5 GHz and notch characteristic from 5 to 6 GHz. In Figs. 10 and 11, the WLAN center frequency somewhat varies with W_3 and W_4, but the major variation is in the WiMAX center frequency. Their values were chosen as 0.7 mm and 0.3 mm, respectively, to have the center frequency at 3.5 GHz.

The notches lengths also have effects on the notches operation. In Fig. 12, the effect of varying the length of the WLAN notch filter is illustrated. As expected, as the length changes, the center frequency of the WLAN changes too, while the center frequency of WiMAX is fixed. The value was chosen to be 15.8 mm. Figures 13 and 14 illustrate the effect of varying the lengths L_3 and L_4 (the total length of the WiMAX notch). The values of L_3 and L_4 mainly affect the center frequency of the WiMAX, while the center frequency of the WLAN is slightly affected. The optimum values were chosen 6 mm and 14 mm, respectively, where the sum of L_3 and L_4 is the same as the total length of the WiMAX notch computed using Equation (2).

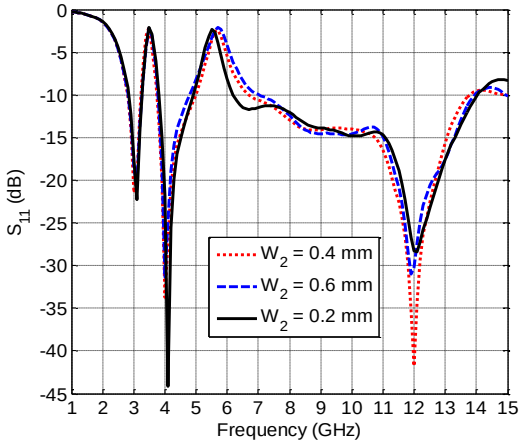

Fig. 9. The effect of varying the value of W_2 with W_3 = 0.7 mm, W_4 = 0.3 mm, and optimum notches lengths.

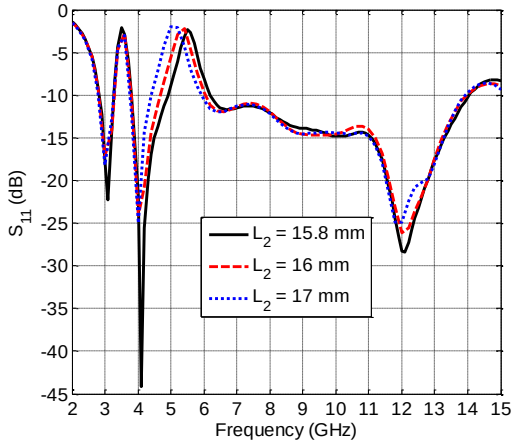

Fig. 12. The effect of varying the value of L_2 with L_3 = 6 mm, L_4 = 14 mm and optimum notches widths.

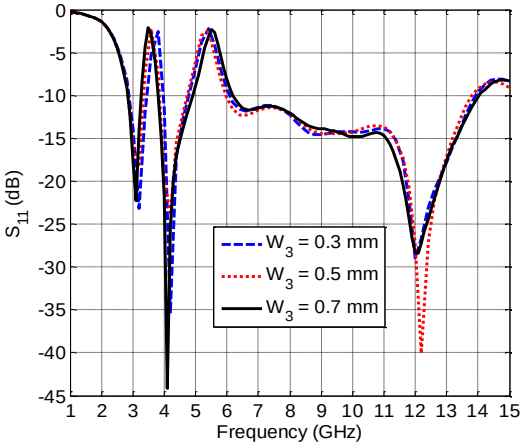

Fig. 10. The effect of varying the value of W_3 with W_2 = 0.2 mm, W_4 = 0.3 mm and optimum notches lengths.

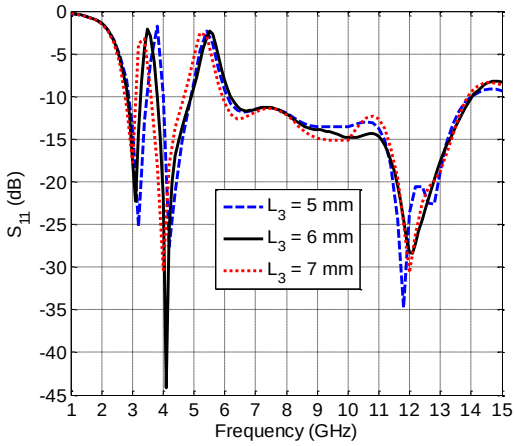

Fig. 13. The effect of varying the value of L_3 with L_2 = 15.8 mm, L_4 = 14 mm and optimum notches widths.

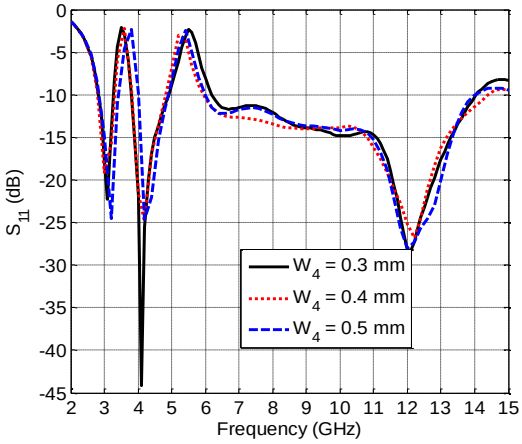

Fig. 11. The effect of varying the value of W_4 with W_2 = 0.2 mm, W_3 = 0.7 mm and optimum notches lengths.

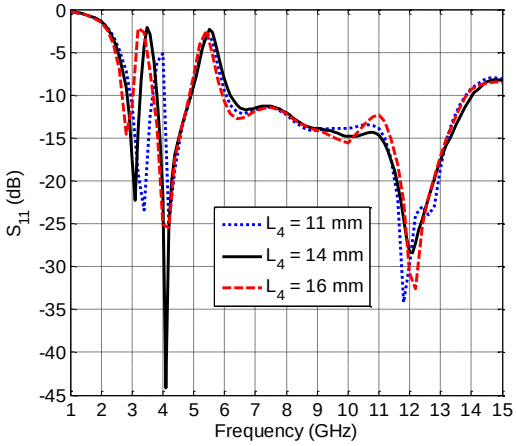

Fig. 14. The effect of varying the value of L_4 with L_2 = 15.8 mm, L_3 = 6 mm and optimum notches widths.

V. CONCLUSIONS

In this paper, a simple printed monopole UWB antenna with two band-notched frequencies was designed and analyzed. Simulations showed that the antenna works well in the UWB range with better than 10 dB return loss. Experimental results were very close to the simulation ones. Frequency domain and time domain characteristics were investigated. The antenna exhibits an omni-directional radiation pattern with high peak gain except at the notched frequencies. Also, the group delay of the antenna was almost constant such that the distortion caused by the antenna is very small except at the notched frequencies. The advantages of the proposed antenna are: cheap, simple and compact for small portable devices. Additionally, the proposed antenna has stable radiation characteristics and can reject interference from existing wireless systems working in the same band of frequencies.

REFERENCES

[1] Federal Communications Commission, First Report and Order, Revision of Part 15 of Commission's Rule Regarding UWB Transmission System FCC 02-48, Washington, DC, USA, 2002.

[2] R. Azim and M. T. Islam, "Ultra-wideband planar antenna with notched bands at 3.5/5.5 GHz," *ACES Journal*, vol. 31, no. 4, pp. 388-395, April 2016.

[3] S. Ojaroudi, Y. Ojaroudi, N. Ghadimi, and N. Ojaroudi, "UWB monopole antenna with dual band-stop performance using G-shaped SRR and SIR structures at feed line," *ACES Journal*, vol. 29, no. 10, pp. 807-812, October 2014.

[4] R. V. R. Krishna, R. Kumar, and N. Kushwaha, "An UWB dual polarized microstrip fed L-shape slot antenna," *International Journal of Microwave and Wireless Technologies*. Available on: CJO2015. doi:10.1017/S1759078715000124

[5] J. Zolghadr, Y. Cai, and N. Ojaroudi, "UWB slot antenna with band-notched property with time domain modeling based on genetic algorithm optimization," *ACES Journal*, vol. 31, no.8, pp. 926-932, August 2016.

[6] A. A. Omar, "Design of ultra-wideband coplanar waveguide-fed Koch-fractal triangular antenna," *International Journal of RF and Microwave Computer-Aided Engineering*, vol. 23, pp. 200-207, 2013.

[7] A. Nemati and B. A. Ganji, "UWB monopole antenna with switchable band-notch characteristic using a novel MEMS afloat," *ACES Journal*, vol. 30, no. 12, pp. 1306-1312, December 2015.

[8] J. Mazloum and N. Ojaroudi, "Utilization of protruded strip resonators to design a compact UWB antenna with WiMAX and WLAN notch bands," *ACES Journal*, vol. 31, no. 2, pp. 204-209, February 2016.

[9] M. Devi, A. K. Gautam, and B. K. Kanaujia, "A compact ultra wideband antenna with triple band-notch characteristics," *International Journal of Microwave and Wireless Technologies*. Available on: CJO2015.doi: 10.1017/S1759078715000409

[10] S. Trinh-Van and Ch. Dao-Ngoc, "Dual band-notched UWB antenna based on electromagnetic band gap structures," *REV Journal on Electronics and Communications*, vol. 1, no. 2, pp. 130-136, April-June 2011.

[11] H. J. Lak, C. Ghobadi, and J. Nourinia, "A novel ultra-wideband monopole antenna with band-stop characteristic," *Wireless Engineering and Technology*, vol. 2, pp. 235-239, 2011.

[12] Y.-S. Li, X.-D. Yang, Q. Yang, and C.-Y. Liu, "Compact coplanar waveguide fed ultra wideband antenna with a notch band characteristic," *International Journal of Electronics and Communications*, vol. 65, no. 11, pp. 961-966, 2011.

[13] J. Zang and X. Wang, "A compact C-shaped printed UWB antenna with band-notched characteristic," *Progress In Electromagnetics Research Letters*, vol. 43, pp. 15-23, 2013.

[14] M. Ojaroudi, G. Ghanbari, N. Ojaroudi, and C. Ghobadi, "Small square monopole antenna for UWB applications with variable frequency band-notch function," *IEEE Antennas and Wireless Propagation Letters*, vol. 8, pp. 1061-1064, 2009.

[15] P. Lotfi, S. Soltani, and M. Azarmanesh, "Triple band-notched UWB CPW and microstrip line fed monopole antenna using broken ∩-shaped slot," *International Journal of Electronics and Communications*, vol. 67, pp. 734-741, 2013.

[16] Z. Yu, G. Wang, J. Liang, and X. Gao, "A semicircular band-notch ultra wideband printed antenna based on CSRR," *Microwave and Optical Technology Letters*, vol. 52, no. 10, pp. 2387-2390, October 2010.

[17] I. Messaoudene, T. A. Denidni, and A. Benghalia, "A hybrid integrated ultra-wideband/dual-band antenna with high isolation," *International Journal of Microwave and Wireless Technologies.* Available on: CJO2015.doi:10.1017/S1759078715000033

[18] M. Yazdi and N. Komjani, "A compact band-notched UWB planar monopole antenna with parasitic elements," *Progress In Electromagnetics Research Letters*, vol. 24, pp. 129-138, 2011.

[19] J. Liang, Ch. Chiau, X. Chen, and C.-G. Parini, "Study of a printed circular disc monopole antenna for UWB systems," *IEEE Transactions on Antennas and Propagations*, vol. 53, no. 11, pp. 3500-3504, November 2005.

[20] T. Wu, H. Bai, P. Li, and X. Shi, "A simple planar monopole UWB slot antenna with dual independently and reconfigurable band-notched characteristics," *International Journal of RF and Microwave Computer-Aided Engineering*, vol. 24, pp. 706-

712, November 2014.
[21] S. Mumby and J. Yuan, "Dielectric properties of FR-4 laminates as a function of thickness and the electrical frequency of the measurement," *Journal of Electronic Materials*, vol. 18, iss. 2, pp. 287-292, March 1989.
[22] C. Balanis, *Antenna Theory: Analysis and Design*, 3rd edition, Wiley Interscience, 2005.
[23] S. Singhal and A. Singh, "Crescent-shaped dipole antenna for ultra-wideband applications," *Microwave and Optical Technology Letters*, vol. 57, iss. 8, pp. 1773-1782, August 2015.
[24] K. Sawant and C. R. Kumar, "CPW fed hexagonal microstrip fractal antenna for UWB wireless communications," *International Journal of Electronics and Communications*, vol. 69, pp. 31-38, 2015.

Shaimaa' A. Naser obtained her B.Sc. in Communications and Electronics Engineering from Jordan University of Science and Technology (JUST), Jordan in 2013. In the same year, she joined the Master program in the Electrical Engineering Department at JUST majoring in Wireless Communications. She obtained her M.Sc. degree in 2015. Her main research interests are in the analysis and design of antennas.

Nihad I. Dib obtained his B.Sc. and M.Sc. in Electrical Engineering from Kuwait University in 1985 and 1987, respectively. He obtained his Ph.D. in EE (major in Electromagnetics) in 1992 from University of Michigan, Ann Arbor. Then, he worked as an Assistant Research Scientist in the Radiation Laboratory at the same school. In Sep. 1995, he joined the EE Department at Jordan University of Science and Technology (JUST) as an Assistant Professor and became a Full Professor in Aug. 2006. His research interests are in computational electromagnetics, antennas and modeling of planar microwave circuits.